Journal on Oncology

www.journalononcology.org

Research Article

Open Access, Volume 6

Preoperative Prediction of Macro Trabecular-Massive Hepatocellular Carcinoma: Value of Ultrasound and Contrast-Enhanced Ultrasound

Yuanqing Zhang[1,2,3]; Yang He[4]; Yifei Chen[4]; Xiaorong Lv[1,2,3]; Yong Yang[1,2,3]; Guo Chen[1,2,3]; Fang Nie[1,2,3]*

[1]Ultrasound Medicine Center, The Second Hospital of Lanzhou University, Lanzhou 730030, Gansu Province, China.

[2]Ultrasound Center, Gansu Provincial Clinical Research Center for Ultrasound Medicine, Lanzhou 730030, Gansu Province, China.

[3]Intelligent Ultrasound Center, Gansu Provincial Engineering Research Center for Intelligent Ultrasound Medicine, Lanzhou 730030, Gansu Province, China.

[4]Lanzhou University, China.

Abstract

Objective: The objective of this study was to develop and validate a predictive model for MTMHCC by integrating preoperative Ultrasound (US) and Contrast-Enhanced Ultrasound (CEUS) features with relevant clinical characteristics.

Methods: This retrospective study analyzed data from patients with histopathological confirmed hepatocellular carcinoma who underwent preoperative CEUS examination at the Ultrasound Department of the Lanzhou University Second Hospital between December 2021 and March 2025. The study cohort comprised 45 patients diagnosed with MTM-HCC and 194 patients with non MTM-HCC. Ultrasound and CEUS images were independently reviewed by two senior abdominal radiologists with extensive experience in hepatic imaging, ensuring objective feature assessment. Clinical variables and imaging characteristics were systematically compared between the two groups to identify distinguishing patterns. To evaluate the associations among clinical data, ultrasound-derived features, and MTM-HCC, univariate analyses were first performed, followed by multivariate logistic regression to construct and assess predictive models.

Results: A total of 239 patients (mean age: 57.28±9.60 years; 187 males and 52 females) were included in the analysis. Among them, 45 HCC patients (18.8%) were classified as the MTM subtype. Multivariate analysis identified four independent predictors: elevated Alpha-Fetoprotein (AFP) (OR=1.01, 95% CI: 1.01-1.11, P<0.001), presence of non-enhancing necrotic areas (OR=5.92, 95% CI: 1.82-19.30, P=0.003), intratumorally arteries (OR=6.61, 95% CI: 2.28-19.22, P<0.001), and peritumoral feeding arteries (OR=3.13, 95% CI: 1.15-8.50, P=0.025).

Conclusion: An integrated prediction model that combines ultrasound imaging and clinical parameters offers a feasible, non-invasive approach for accurate preoperative identification of MTM-HCC.

Keywords: Ultrasound-contrast; Liver; Macro trabecular-massive hepatocellular carcinoma; Contrast-enhanced ultrasound Preoperative prediction.

Manuscript Information: *Received: Feb 01, 2026; Accepted: Feb 26, 2026; Published: Mar 05, 2026*

Correspondance: *Fang Nie, Ultrasound Medicine Center, The Second Hospital of Lanzhou University, Chengguan District, Lanzhou City, Gansu Province, China. Email: ery-nief@lzu.edu.cn*

Citation: *Zhang Y, He Y, Chen Y, Lv X, Nie F, et al. Preoperative Prediction of Macro Trabecular-Massive Hepatocellular Carcinoma: Value of Ultrasound and Contrast-Enhanced Ultrasound. J Oncology. 2026; 6(1): 1199.*

Introduction

Liver cancer remains a major global health burden, ranking as the third leading cause of cancer related mortality worldwide [1,2]. The burden is especially heavy in East Asia, where nearly half of all global liver cancer cases and deaths occur in China [2]. Among primary liver cancers, Hepatocellular Carcinoma (HCC) accounts for the most significant proportion and is the most common pathological type encountered in clinical practice [3,4]. Chronic infection with Hepatitis B Virus (HBV) or Hepatitis C Virus (HCV) significantly elevates HCC risk, primarily through sustained inflammation and fibrogenesis that promote carcinogenesis [5]. In addition to viral causes, long-term alcohol consumption accelerates liver damage and increases the likelihood of cirrhosis and HCC, especially at high intake levels, and Nonalcoholic Steatohepatitis (NASH)-the progressive form of nonalcoholic fatty liver disease associated with obesity and metabolic syndrome-has emerged as a significant risk factor for HCC development [5]. The development of hepatocellular carcinoma is closely linked to chronic liver injury and a spectrum of established risk factors. Liver cirrhosis, regardless of etiology, remains the most important premalignant condition [5]. The high heterogeneity of HCC at genomic and histopathological levels limits the effectiveness of treatment strategies based solely on clinical staging systems such as the Barcelona Clinic Liver Cancer (BCLC) [6]. The World Health Organization (WHO) Classification of Tumours categorizes HCC into eight distinct pathological subtypes [7]. Among the recognized histological subtypes of HCC, the Macro Trabecular- Massive (MTM) variant has attracted particular attention because of its distinctly aggressive biological and molecular profile. This subtype is characterized by marked angiogenesis, frequent vascular invasion, and activation of proliferative signaling pathways, features that collectively underpin its unfavorable clinical course [8]. At present, definitive diagnosis of MTM-HCC still depends on postoperative histopathological assessment of resected tumor specimens [9]. Which limits timely risk stratification and treatment planning in the preoperative setting [10]. In addition to its aggressive clinical behavior, MTM-HCC exhibits distinctive microscopic features. Histopathological, this subtype is characterized by a predominant macro trabecular growth pattern, in which tumor trabeculae exceed six cells in thickness. These thickened trabeculae are composed of compact cords of tumor cells surrounded by endothelial-lined vascular channels, creating a vessel-encapsulating architecture that distinguishes MTM-HCC from conventional trabecular HCC patterns [11,12]. MTM-HCC is characterized by a rich angiogenesis pattern in CD34-positive blood vessels, which includes tumor clusters (vessel-encapsulating tumor clusters). This histological feature is an indicator of poor prognosis, linked to rapid tumor dissemination and a high incidence of early recurrence [10,13]. Accurate preoperative identification of MTM-HCC is of great clinical value for formulating individualized treatment plans and improving patient prognosis. At present, studies on the imaging features of MTM-HCC are still scarce, and there is no consensus on the optimal predictive biomarkers for this subtype. Among existing imaging studies, Mulé et al. [14], reported that extensive tumor necrosis observed in contrast-enhanced Magnetic Resonance Imaging (MRI) is an independent predictive factor for MTM-HCC, which has high specificity in identifying this subtype. Feng et al. [11], confirmed through Computed Tomography (CT) imaging studies that intratumorally hemorrhage and intratumorally necrosis can serve as independent predictive indicators for MTMHCC. While Magnetic Resonance Imaging (MRI) and Computed Tomography (CT) has demonstrated significant diagnostic value for MTM-HCC, it remains constrained by costs and accessibility. More importantly, Contrast-Enhanced Ultrasound (CEUS) offers superior real-time dynamic imaging capabilities, enabling the capture of ultra-early microvascular enhancement features, such as intertumoral arteries, which may be transient or overlooked during the fixed-time phase acquisitions of CT or MRI. This unique advantage positioning CEUS as a highly sensitive and accessible tool for the preoperative identification of tumor aggressiveness. Beyond lesion detection, modern ultrasound techniques-particularly Doppler imaging and contrast-enhanced ultrasound-allow assessment of tissue perfusion, vascular architecture, and hemodynamic behavior, thereby providing functional information closely related to disease biology [5,15]. This real-time capability facilitates a more direct evaluation of tumor microvascular architecture and hemodynamic behavior [16]. For example, Wilson et al. demonstrated that contrast-enhanced ultrasound could accurately characterize focal liver lesions by capturing dynamic vascular patterns, achieving diagnostic performance comparable to cross-sectional imaging [17]. Collectively, these studies suggest that ultrasound is not merely a screening or descriptive tool, but a robust imaging modality capable of supporting preoperative prediction and clinical decision-making. However, systematic studies on the ultrasound features of MTM-HCC are still limited, and the value of CEUS in the preoperative diagnosis of this subtype has not been fully explored [18,19]. Therefore, an urgent need exists to systematically evaluate the potential of preoperative ultrasound features combined with clinical indicators MTM-HCC, and provide a new non-invasive diagnostic approach for the early identification of this aggressive subtype. Accordingly, this study aimed to evaluate the value of ultrasound-based features combined with clinical parameters for the preoperative identification of macro trabecular-massive hepatocellular carcinoma.

Materials and methods

General information: Consecutive patients with Hepatocellular Carcinoma (HCC) who underwent preoperative conventional Ultrasound (US) and CEUS examinations in the Department of Ultrasound at the Second Hospital of Lanzhou University between December 2021 and March 2025 were initially identified. The diagnosis of HCC was histopathological confirmed in all included patients by either surgical resection or biopsy.

For the cohort, consecutive patients with hepatocellular carcinoma confirmed by pathology who underwent preoperative conventional ultrasound and Contrast-Enhanced Ultrasound (CEUS) at our institution were retrospectively reviewed.

Patients were enrolled if they met the following criteria: (1) conventional ultrasound and liver CEUS using Sonovoxes® (Bracco) were performed within 1 month before surgery, (2) the diagnosis of HCC was confirmed by postoperative pathological examination, and (3) no antitumor treatment was administered prior to ultrasound examination.

The exclusion criteria were as follows: (1) poor-quality ultrasound or CEUS images, including incomplete arterial, portal venous, or late phase acquisition, missed lesions, or excessive respiratory motion, (2) an interval of more than 3 months

between ultrasound examination and pathological diagnosis, and (3) incomplete clinical, laboratory, or pathological data. After applying these criteria, a total of 239 patients constituted the final study cohort. The flowchart of patient enrollment and exclusion is shown in (Figure 1).

Examination method: Contrast-Enhanced Ultrasound (CEUS) was performed using a Philips EPIQ7 ultrasound system with a C5-1 convex transducer (1-5 MHz) under a low-mechanical index setting. Following identification of the target lesion, CEUS was obtained; in patients with multiple lesions, the largest lesion and its maximal cross-sectional plane were selected for evaluation. Sonovoxes (Bracco, Milan, Italy) was administered as a 2.4 mL bolus via the antecubital vein, immediately followed by a 5 mL saline flush. CEUS cine loops were acquired continuously in real time and digitally stored for subsequent analysis. All examinations were independently interpreted by two radiologists with more than 5 years of experience in hepatic CEUS, both of whom were blinded to the pathological findings. Histopathological Analysis.

All histological sections were reviewed by a pathologist with 16 years of experience (W.D. Li), who was blinded to other clinical and imaging findings.

Diagnosis was based on previous pathological criteria: (1) The dominant architectural pattern of the tumor is the macro trabecular pattern (with trabecular thickness exceeding six cells) [7,19,20]. (2) The Edmondson-Steiner grade and immunohistochemical markers (Ki-67 index, CD34, Glypican-3, and CK19) were recorded simultaneously.

Image analysis: To ensure the reliability of imaging interpretation, all conventional ultrasound and Contrast Enhanced Ultrasound (CEUS) images were independently reviewed by two ultrasound physicians (With 15 and 13 years of experience in hepatic ultrasound, respectively) who were blinded to the patients' clinical and pathological information. In cases of disagreement, a consensus was reached through joint discussion. For patients with multiple lesions, the largest tumor was selected for evaluation. According to the American College of Radiology CEUS Liver Imaging Reporting and Data System (LI-RADS, version 2017), LI-RADS categories were assigned in 181 of the 239 patients.

The following ultrasound and CEUS characteristics were evaluated for each lesion: (1) number of lesions, (2) maximum tumor diameter, (3) shape, (4) echogenicity, (5) echo homogeneity, (6) tumor margin, (7) tumor capsule, (8) nodule-in-nodule appearance, (9) peritumoral blood flow signal graded according to the Adler classification, (10) arterial phase (AP) enhancement onset time, (11) AP enhancement degree, (12) expansion of the enhanced area in the AP, (13) AP enhancement pattern, (14) washout onset time, (15) portal venous phase (PVP) washout degree, (16) delayed phase clearance pattern, (17) intertumoral necrosis, (18) intertumoral artery, (19) peritumoral feeding artery, and (20) portal vein tumor thrombus.

Statistical analysis

Variables associated with Macro Trabecular-Massive Hepatocellular Carcinoma (MTM-HCC) were first screened using univariate analysis and subsequently entered into multivariable binary logistic regression to identify independent predictors. Serum Alpha-Fetoprotein (AFP) was initially analyzed as a continuous variable in both univariate and multivariable models. For construction of the final combined predictive model, AFP was dichotomized to improve clinical interpretability, with the optimal cutoff determined by Receiver Operating Characteristic (ROC) curve analysis using the Youden index. The dichotomized AFP variable was then incorporated into the model together with selected contrast-enhanced ultrasound features.

ROC curves were used to assess the discriminative performance of the model, and diagnostic efficacy was evaluated by sensitivity, specificity, accuracy, positive predictive value, negative predictive value, and Area Under the ROC Curve (AUC).

Statistical analyses were performed using SPSS 26.0 (IBM, Armonk, NY, USA) and R 4.4.2 (https://www.r-project.org/). Measurement data with normal distribution were expressed as $\bar{x} \pm s$, and comparisons between groups were conducted using the independent samples t-test. Data with non-normal distribution were presented as M (Q1, Q3), and intergroup comparisons were performed using the Mann-Whitney U test. Categorical variables were expressed as frequencies or percentages, and differences between groups were tested using the χ^2 test. A P-value<0.05 was considered statistically significant.

Results

Clinical and pathological baseline data of patients

A total of 239 patients were included in the analysis, comprising 194 patients with non-MTMHCC and 45 patients with MTM-HCC. The two groups were comparable in terms of sex distribution, with no significant difference observed (P=0.751). In contrast, patients with MTM-HCC exhibited markedly elevated serum alpha-fetoprotein (AFP) levels compared with those in the non-MTMHCC group (median, 1210.0 vs. 32.6 ng/mL; P<0.001). Regarding liver function - related parameters, Aspartate Aminotransferase (AST) levels were significantly higher in the MTM-HCC group (P=0.005), whereas no significant differences were observed in alanine aminotransferase (ALT), Albumin (ALB), Total Bilirubin (T-bil), Hemoglobin (Hb), or Platelet counts (PLT) between the two groups. Inflammatory status, patients with MTM-HCC showed higher peripheral neutrophil (NEU) counts (P=0.045) and a significantly increased Neutrophil-To-Lymphocyte Ratio (NLR) (P=0.009), indicating a more pronounced inflammatory response. No significant differences were observed between the two groups in terms of hepatitis B virus (HBV) infection status or the prevalence of liver cirrhosis. From pathological, MTM-HCC was more frequently associated with CK19+ (33.3% vs. 17.0%, P=0.014), higher Edmondson-Steiner grades (III–IV) (33.3% vs. 11.3%, P<0.001), and a significantly higher Ki67 index (median, 40% vs. 30%; P<0.001). In contrast, no significant differences were observed in the expression of CD34 or glypican-3. (Table 1).

Imaging findings of MTM-HCC on US and CEUS

Compared with non-MTM-HCC, MTM-HCC lesions were significantly larger, with a greater maximum tumor diameter (median, 6.6 cm vs. 3.7 cm; P < 0.001) and a higher proportion of tumors larger than 5 cm (30 of 45 [66.7%] vs. 60 of 194 [30.9%], P<0.001). MTM-HCC more frequently exhibited heterogeneous echogenicity (42 of 45 [93.3%] vs. 141 of 194 [72.7%], P=0.003) and indistinct tumor margins (34 of 45 [75.6%] vs. 83 of 194 [42.8%]), P<0.001). The nodule-in nodule sign was more common in MTM-HCC than in

non-MTM-HCC (29 of 45 [64.4%] vs. 81 of 194 [41.8%], P=0.006). On CEUS, MTM-HCC demonstrated less frequent arterial-phase expansion of the enhanced area (3/45 [6.7%] vs. 37/194 [19.1%], P=0.045) but significantly more frequent arterial-phase peripheral nodular enhancement (31/45 [68.9%] vs. 49/194 [25.3%], P<0.001). In the portal venous phase (PVP), MTM-HCC exhibited a more pronounced degree of washout compared with non - MTM-HCC (21 of 45 [46.7%] vs. 60 of 194 [30.9%], P=0.027). MTM-HCC more commonly exhibited non-enhancing necrotic areas compared with non-MTM-HCC (30/45 [66.7%] vs. 46/194 [23.7%], P<0.001). Intertumoral arteries were more frequently observed in MTM-HCC (33 of 45 [73.3%] vs. 45 of 194 [23.2%], P<0.001), as were peritumoral feeding arteries (28 of 45 [62.2%] vs. 70 of 194 [36.1%], P=0.001). Moreover, the incidence of venous tumor thrombus was significantly higher in MTM-HCC compared with non-MTM-HCC (21/45 [46.7%] vs. 39/194 [20.1%], P<0.001). (Table 2).

Development of a predictive model for MTM-HCC

In multivariable logistic regression analysis, elevated serum AFP levels were independently associated with the MTM subtype (OR=1.01, 95% CI: 1.01-1.11; P<0.001). Among imaging features, non-enhancing necrotic areas (OR=5.92, 95% CI: 1.82-19.30; P=0.003), intratumoral arteries (OR=6.61, 95% CI: 2.28-19.22; P<0.001), and the presence of a peritumoral feeding artery (OR=3.13, 95% CI: 1.15-8.50; P=0.025) were independently associated with MTM-HCC (Table 3).

By integrating clinical variables and CEUS features using a multivariable logistic regression approach, a combined prediction model was established for identifying the MTM subtype of HCC (variables: AFP＞467 ng/mL, non-enhanced intratumorally necrosis, intratumorally artery, and peritumoral feeding artery).

Using multivariable logistic regression, we developed a combined model to predict the MTM subtype of Hepatocellular Carcinoma (HCC). This model integrates three contrast-enhanced ultrasound features and an Alpha-Fetoprotein (AFP) level ＞467 ng/mL. In the training cohort, the model showed strong performance, with an Area Under the Curve (AUC) of 0.91 (95% CI: 0.860-0.970; Figure 3A), a sensitivity of 88.9%, and a specificity of 71.6%. The calibration curve indicated close agreement between the predicted risk and the actual outcomes (Figure 3B).

Table 1: Clinical and histopathological characteristics of patients between the two groups.

Characteristic	Non-MTM-HCC (n=194)	MTM-HCC (n=45)	P				
	Sex, n (%)	0.751					
Female	43 (22.16)	9 (20.00) males	151 (77.84)	36 (80.00) age/Year	57.60±9.37	55.91±10.57	0.288
	AFP (ng/mL)	32.55 (4.29, 261.60)	1210.00 (475.00, 1210.00)	<.001			
	CA199(U/mL)	18.25 (9.19, 38.82)	23.90 (12.70, 45.10)	0.304			
	ALT(U/L)	41.00 (25.25, 114.75)	49.00 (33.00, 151.00)	0.152			
	AST(U/L)	56.50 (37.00, 140.50)	100.00 (53.00, 215.00)	0.005			
	ALB(g/L)	36.00 (31.90, 40.10)	36.70 (34.00, 38.10)	0.955			
	TBIL (μmol/l)	22.75 (16.15, 33.70)	25.40 (19.20, 34.50)	0.437			
	Hb(g/L)	143.00 (124.00, 156.50)	144.00 (119.00, 154.00)	0.828			
	PLT (×10^9/l)	132.00 (88.25, 190.00)	152.00 (112.00, 192.00)	0.105			
	N (×10^9/l)	4.16 (2.31, 6.72)	5.24 (3.49, 7.36)	0.045			
	L (×10^9/l)	1.03 (0.70, 1.50)	0.84 (0.66, 1.32)	0.078			
	NLR	3.62 (2.16, 8.03)	5.19 (3.31, 14.00)	0.009			
	HBV, n (%)	0.677					
	No	46 (23.71)	12 (26.67)				
	Yes	148 (76.29)	33 (73.33)				
	liver cirrhosis, n (%)	0.910					
	No	49 (25.26)	11 (24.44)				
	Yes	145 (74.74)	34 (75.56)				
	CD34, n (%)	0.577					
16 (8.25)	2 (4.44)						
	+	178 (91.75)	43 (95.56)				
	Glypican3, n (%)	0.329					
38 (19.59)	6 (13.33)						
	+	156 (80.41)	39 (86.67)				
	CK19, n (%)	0.014					
161 (82.99)	30 (66.67)						
	+	33 (17.01)	15 (33.33)				
	Edmonson-Steiner Grade (I-II/III-IV), n (%)	<.001					
	I-II	172 (88.66)	30 (66.67)				
	III-IV	22 (11.34)	15 (33.33)				
	Ki67(%)	30.00 (20.00, 40.00)	40.00 (30.00, 60.00)	<.001			

Unless otherwise specified, data are presented as median with interquartile range in parentheses.
Abbreviations: MTM: Thick Trabecular-Mass type; HCC: Hepatocellular Carcinoma; AFP: Alpha-Fetoprotein; CA199: Carbohydrate Antigen 199; ALT: Alanine Aminotransferase; AST: Aspartate Aminotransferase; ALB: Albumin; TBIL: Total Bilirubin; Hb: Hemoglobin; PLT: Platelet; N: Neutrophil: L : Lymphocyte; NLR: Neutrophil/lymphocyte ratio; HBV: Hepatitis B virus.
a: Data are presented as mean ± standard deviation; b: Data are presented as number of patients; data in parentheses are percentages.

Table 2: Comparison results of US and CEUS features between the two groups of patients characteristics Non-MTM-HCC (n=194) MTM-HCC (n = 45) P.

Number of tumors, n (%)			**0.133**
Isolated	93 (47.94)	16 (35.56)	
Multiple	101 (52.06)	29 (64.44)	
Echo, n (%)			0.599
Hypoechoic	124 (63.92)	31 (68.89)	
isoechoic	9 (4.64)	1 (2.22)	
Mixed echo	15 (7.73)	1 (2.22)	
Hyperechoic	46 (23.71)	12 (26.67)	
Maximum diameter (cm)	3.70 (2.20, 5.47)	6.60 (3.80, 8.20)	<.001
Size classification, n (%)			<.001
＜3cm	73 (37.63)	7 (15.56)	
2.3-5cm	61 (31.44)	8 (17.78)	
＞5cm	60 (30.93)	30 (66.67)	
Echo homogeneity, n (%)			0.003
Uniform	53 (27.32)	3 (6.67)	
Non-uniform	141 (72.68)	42 (93.33)	
CDFI, n (%)			0.093
Grade 0	41 (21.13)	5 (11.11)	
Grade I	62 (31.96)	10 (22.22)	
Grade II	6 (3.09)	1 (2.22)	
Grade III	85 (43.81)	29 (64.44)	
Morphology, n (%)			0.267
Regular	149 (76.80)	31 (68.89)	
Irregular	45 (23.20)	14 (31.11)	
Tumor margin, n (%)			<.001
Clear	111 (57.22)	11 (24.44)	
Indistinct	83 (42.78)	34 (75.56)	
Encapsulation, n (%)			0.070
Yes	98 (50.52)	16 (35.56)	
No	96 (49.48)	29 (64.44)	
Knot within a knot, n (%)			0.006
Yes	81 (41.75)	29 (64.44)	
No	113 (58.25)	16 (35.56)	
AP Start Enhancement Time	15.00 (13.00, 18.00)	15.00 (14.00, 17.00)	0.820
(s)			
Whether Range Expanded			
After Enhancement, n (%)			**0.045**
Yes	37 (19.07)	3 (6.67)	
No AP Enhancement Pattern,	157 (80.93)	42 (93.33)	
N (%)			0.777
High Enhancement	171 (88.14)	42 (93.33)	
Isotopic Enhancement	20 (10.31)	3 (6.67)	
Low Enhancement Arterial Phase Enhancement	3 (1.55)	0 (0.00)	
Pattern, n (%)			<.001
Synchronous Enhancement Peripheral Nodular	116 (59.79)	8 (17.78)	
Enhancement	49 (25.26)	31 (68.89)	
Annular Enhancement	11 (5.67)	2 (4.44)	
Centrifugal Enhancement	18 (9.28)	4 (8.89)	
Start of Decay Time, n (%)			0.226
Ultra-Early Decay (＜30s)	8 (4.12)	4 (8.89)	
Early Decay (＜60s)	68 (35.05)	20 (44.44)	
Late Decay (＞60s)	118 (60.83)	21 (46.67)	
PVP Decay Degree, n (%)			0.027
No Decay	56 (28.87)	5 (11.11)	
Mild Decay	78 (40.21)	19 (42.22)	
Marked Decay	60 (30.93)	21 (46.67)	
DP Clearance Degree, n (%)			0.127
No Clearance	28 (14.43)	2 (4.44)	
Incomplete Clearance	88 (45.36)	18 (40.00)	
Complete Clearance No enhancement in necrotic	78 (40.21)	25 (55.56)	
areas, n (%)			<.001
No	148 (76.29)	15 (33.33)	
Yes	46 (23.71)	30 (66.67)	
Intramodular artery, n (%)			<.001
No	149 (76.80)	12 (26.67)	
Yes	45 (23.20)	33 (73.33)	
FA, n (%)			0.001
No	124 (63.92)	17 (37.78)	
Yes	70 (36.08)	28 (62.22)	
VTT, n (%)			<.001
No	155 (79.90)	24 (53.33)	
Yes	39 (20.10)	21 (46.67)	
LI-RADS, n (%)			0.746
3	5 (3.38)	0 (0.00)	
4	30 (20.27)	5 (15.15)	
5	99 (66.89)	24 (72.73)	
M	14 (9.46)	4 (12.12)	

Note: Data are presented as number of patients, with percentages in parentheses.
This study only included high-risk populations meeting the criteria of CEUS LI-RADS 2017, i.e., participants with cirrhosis, Hepatitis B Virus (HBV) infection, or a history of Hepatocellular Carcinoma (HCC), totaling 181 (derived from 239 initially enrolled patients).
Abbreviations: CDFI: Color Doppler Flow Imaging features; MTM: Thick Trabecular-Mass type; HCC: Hepatocellular carcinoma; AP: Arterial Phase; PVP: Portal Venous Phase<120s; DP: Delayed Phase; FA Peritumoral Feeding Artery; VTT: Venous Tumor Thrombus.
a. Data are presented as median, with interquartile range in parentheses.

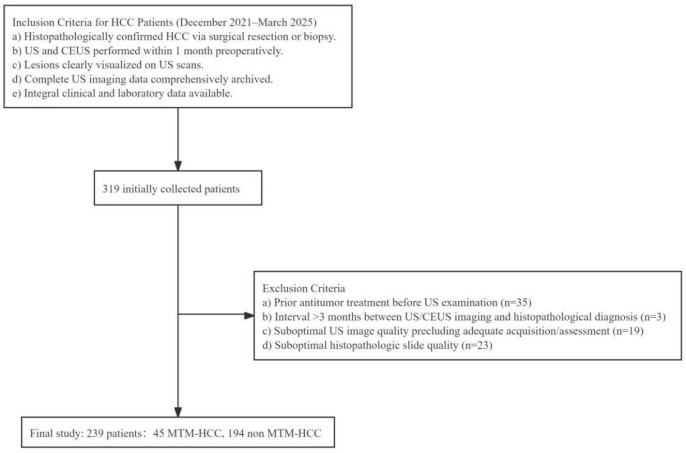

Figure 1: Flow diagram for patient enrollment in this study. US: Conventional Ultrasound; CEUS: Contrast-Enhanced Ultrasound; HCC: Hepatocellular Carcinoma; MTM-HCC: Thick Trabecular-Mass Type Hepatocellular Carcinoma.

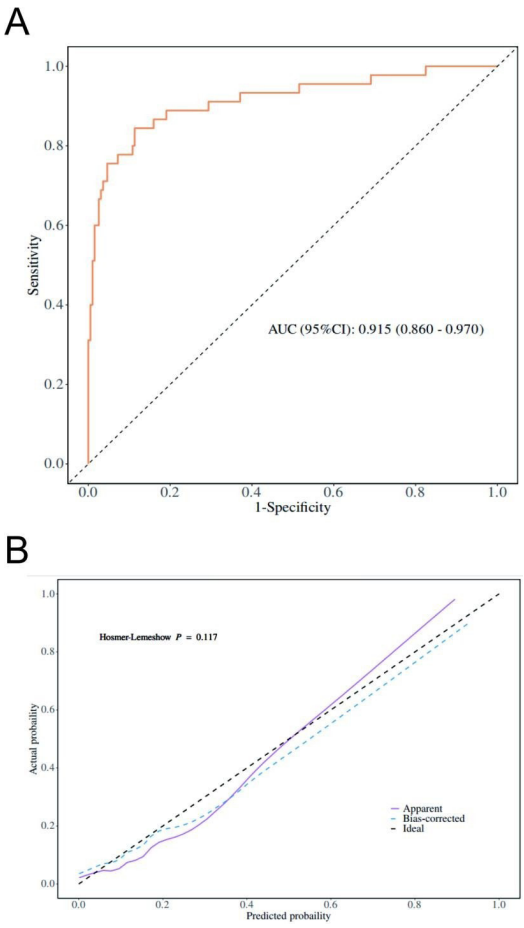

Figure 3: Predictive performance and calibration of the Contrast-Enhanced Ultrasound (CEUS)-clinical model for MTM-HCC. **(A)** The Area Under the Curve (AUC) in the training cohort was 0.91 (95% confidence interval [CI]: 0.860-0.970). **(B)** The optimal cut-off value is 0.255, with corresponding sensitivity of 88.9%, specificity of 71.6%, Negative Predictive Value (NPV) of 97.0%, Positive Predictive Value (PPV) of 38.7%, and accuracy of 74.5%. The calibration curve agrees closely with the predicted curve after calibration.

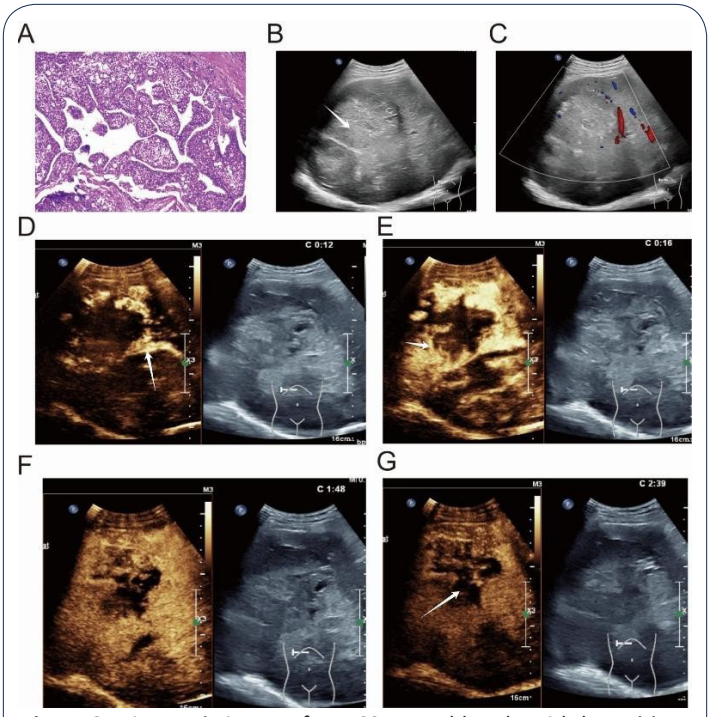

Figure 2: Diagnostic images for a 60-year-old male with hepatitis B virus-related cirrhosis and Macro Trabecular-Massive Hepatocellular Carcinoma (MTM-HCC). Laboratory data showed an AFP level of 1210 ng/mL, AST 65 U/L, and Neutrophil-To-Lymphocyte Ratio (NLR) > 6. Pathological immunohistochemistry demonstrated a Ki-67 index of 60%. **(A)** Micrograph reveals a macro trabecular-massive growth pattern. **(B)** Two-dimensional ultrasound image demonstrates an approximately 8.7-cm HCC in segment VIII of the right hepatic lobe. The mass exhibits heterogeneous echogenicity, a peripheral hypoechoic halo, and a "nodule-in-nodule" appearance. The lesion is indicated by white arrows. **(C)** Peripheral rim-like blood flow signals are observed around the mass. **(D-G)**: Preoperative contrast-enhanced ultrasound (CEUS) images. **(D,E)**: In the arterial phase, the lesion shows peripheral nodular hyperenhancement. intratumorally arteries **(D)** and peritumoral arteries **(E)** are visible, each marked by white arrows. **(F)** In the portal venous phase, the lesion exhibits marked washout, appearing hypoechoic. 9G) In the delayed phase, the lesion shows sustained hypo-enhancement. Non-enhancing necrotic areas are present throughout all phases. According to the CEUS Liver Imaging Reporting and Data System (CEUS LI-RADS) 2017, this nodule was classified as LR-M.

Discussion

This study demonstrates that the combination of serum Alpha-Fetoprotein (AFP) with specific Contrast-Enhanced Ultrasound (CEUS) features - non-enhanced necrosis within the tumor, intratumorally arteries, and peritumoral feeding arteries - can reliably identify the Microvascular Invasion (MTM) subtype of Hepatocellular Carcinoma (HCC) preoperatively. By integrating these four features into a CEUS-clinical model, we have established a non-invasive preoperative prediction method for MTM-HCC. Notably, the incidence of MTM-HCC observed in our cohort (45 out of 239 cases, 18.8%) is very close to the rates reported in previous studies [14,18,21], supporting the representativeness of our sample. These findings are consistent with the pathological hallmarks of MTM-HCC, which include thick macro trabecular architecture, marked angiogenesis, and vessel encapsulating tumor clusters [22,23]. Such features correspond to increased arterial supply and

Table 3.1: Analysis of predictors in binary logistic regression for MTM-HCC.

Variable	P-value of univariate analysis	P-value of multivariate analysis	Multivariate OR (95% CI)
AFP≥467 ng/mL	<.001	<.001	1.01 (1.01 ~ 1.01)
AST	0.575	0.334	1.00 (1.00 ~ 1.00)
N	0.656	0.509	0.97 (0.88 ~ 1.07)
NLR	0.128	0.054	1.06 (1.00 ~ 1.13)
Maximum tumor diameter	<.001	0.529	0.93 (0.74 ~ 1.17)
Tumor size classification	<.001	0.528	0.72 (0.27 ~ 1.97)
Echogenicity homogeneity	0.007	0.191	3.20 (0.56 ~ 18.29)
Tumor margins	<.001	0.392	1.60 (0.54 ~ 4.71)
Double-peaked enhancement pattern	0.007	0.513	0.71 (0.26 ~ 1.97)
Enhanced area	0.056	0.178	3.09 (0.60 ~ 15.91)
Arterial phase enhancement pattern	0.011	0.684	0.90 (0.53 ~ 1.51)
Degree of PVP washout	0.009	0.896	0.95 (0.43 ~ 2.09)
Necrotic areas without enhancement	<.001	0.003	5.92 (1.82 ~ 19.30)
Intramural arteries	<.001	<.001	6.61 (2.28 ~ 19.22)
FA	0.002	0.025	3.13 (1.15 ~ 8.50)
VTT	<.001	0.961	1.03 (0.31 ~ 3.41)

Note: Data in parentheses are 95% confidence intervals.
Abbreviations: MTM: Thick Trabecular-Mass Type; HCC: Hepatocellular Carcinoma; AFP: Alpha-Fetoprotein; AST: Aspartate Aminotransferase; NLR: Neutrophil/lymphocyte Ratio; AP: Arterial Phase; PVP: Portal Venous Phase <120s); FA: Peritumoral Feeding Artery; VTT: Venous Tumor Thrombus; OR: Odds Ratio; CI: Confidence Interval.

Table 3.2: Confusion matrix.

AUC (95% CI)	Accuracy (95% CI)	Sensitivity (95% CI)	Specificity (95% CI)	PPV (95% CI)	NPV cut (95% CI) off
0.915 (0.860-0.970)	0.879 (0.830-0.917)	0.887 (0.842-0.931)	0.844 (0.739-0.950)	0.961 (0.932-0.989)	0.633 (0.511-0.255 0.755)

Note: AUC: Area Under the Curve; PPV: Positive Predictive Value; NPV: Negative Predictive Value; cut-off: critical value.

disorganized tumor vasculature, explaining the frequent presence of intratumorally and peritumoral arteries on CEUS, as reflected in prior imaging-pathology correlation studies [24]. Rapid tumor growth and vascular insufficiency may further lead to hypoxia and intratumorally necrosis, which has been previously described as a common imaging and pathologic correlate of aggressive MTM tumors [24]. Elevated AFP likely reflects the aggressive biological behavior and poor differentiation commonly observed in MTM-HCC [21,25].

Formally recognized by the World Health Organization in 2019, MTM-HCC has attracted growing research attention because its aggressive biological behavior is consistently linked to early recurrence and unfavorable survival outcomes [7,21,26]. From a preoperative standpoint, this creates a practical dilemma: although histopathology remains the diagnostic gold standard, therapeutic decisions often rely on imaging and laboratory data obtained before surgery. Consistent with previous reports [27]. MTM-HCC patients in our cohort more frequently exhibited markedly elevated AFP levels, with nearly two-thirds (29 of 45) exceeding 1000 ng/mL, a range that in routine clinical practice often raises suspicion for biologically aggressive disease.

Higher AST levels were observed in patients with MTM-HCC, likely reflecting tumor-related hepatic injury associated with aggressive tumor growth rather than nonspecific inflammatory changes, as elevated AST has been linked to more extensive tumor necrosis and worse liver function in aggressive HCC subtypes [28]. Pathologically, MTM-HCC lesions exhibited poorer differentiation and increased proliferative activity, as indicated by consistently higher Edmondson-Steiner grades and elevated Ki-67 indices in MTM-HCC compared with non-MTM cases, supporting its hyperproliferative biology [29]. These clinicopathological features are consistent with prior reports describing MTM-HCC as a biologically aggressive subtype characterized by rapid growth, invasive behavior, and a strong propensity for early dissemination [21].

The vascular features identified in this study further reinforce current biological understanding of MTM-HCC. Angiogenesis has been repeatedly described as a defining hallmark of this subtype, with molecular studies highlighting upregulation of angiogenic pathways and overexpression of Ang-2 and VEGFA [20,22,30]. In parallel with these molecular observations, intratumorally arteries emerged as an independent predictor of MTM-HCC in our analysis, consistent with prior imaging-based reports [8,11,18]. From a structural perspective, the macro trabecular architecture-defined by tumor trabeculae exceeding six cells in thickness and dominating the tumor mass-places substantial metabolic and perfusion demands on growing hepatocellular carcinoma. Such thickened trabeculae and associated architectural changes have been consistently described in MTM-HCC histology and are linked to aggressive tumor biology [20]. As malignant hepatocytes expand and replace normal parenchyma, the tumor increasingly relies on arterial blood supply, often resulting in arterialization and distortion of adjacent hepatic arterial branches and abnormal neovascular patterns to meet these demands. This vascular remodeling and increased arterial input likely underpin the frequent imaging observations of prominent intratumorally and peritumoral arterial features in MTM-HCC on contrast-based modalities [24]. In this setting, the presence of peritumoral feeding arteries, also identified as an independent predictor in our model, likely reflects

this heightened vascular dependence. Such hypervascularity may partly explain the propensity of MTMHCC to present as large, poorly encapsulated masses with a high risk of vascular invasion, recurrence, and metastasis [13,31,32].

Such tumor-driven vascular remodeling is expected to translate into distinct perfusion patterns on contrast-enhanced ultrasound. Perfusion behavior on CEUS provided additional insight. In line with earlier investigations [18,19,33], the majority of MTM-HCC lesions in our cohort (40 of 45 cases) demonstrated hypo enhancement during the portal venous phase, frequently accompanied by pronounced washout. When washout degree was stratified, significant washout was more commonly observed in MTM-HCC, suggesting altered tumor hemodynamics. The underlying pathophysiology likely reflects a combination of factors, including early venous drainage and reduction of portal venous blood flow, which predispose lesions to relative hypo enhancement in the portal venous phase compared with background liver parenchyma [34,35]. In addition, rapid tumor proliferation and tightly packed cellularity reduce extracellular volume and limit intratumorally portal perfusion, contributing to more rapid and pronounced contrast washout [36]. Although the precise mechanisms remain incompletely understood, this multifactorial model aligns with prior imaging-pathology correlation studies in HCC, which have proposed that washout reflects the combined effects of reduced nodular portal supply, early venous drainage of contrast, and progressive background liver enhancement. (Yang HK, Burns PN, Jang HJ, et al. [37].

Several limitations merit consideration. The retrospective, single-center design may introduce unavoidable selection bias, and the limited sample size-particularly the small number of MTMHCC cases-restricts the statistical power of subgroup analyses and precludes formal external validation. In addition, the AFP cutoff of 467 ng/mL was derived from ROC analysis within the study cohort; although this improved clinical interpretability, it reflects a data-driven choice that may limit generalizability. Therefore, these findings should be interpreted cautiously and require confirmation in larger, multicenter cohorts. In summary, MTM-HCC demonstrates distinct ultrasound and contrast-enhanced ultrasound features that mirror its aggressive biological profile. By integrating intratumorally necrosis, intratumorally and peritumoral arterial features with serum AFP levels, we established a non-invasive model with good performance for preoperative identification of the MTM subtype. The observed imaging patterns are consistent with the pathological hallmarks of MTM-HCC, including dense macro trabecular architecture and prominent angiogenesis. Collectively, our results suggest that combining CEUS-derived features with readily available clinical markers may aid early risk stratification and support more individualized treatment planning.

Declarations

Ethical statement: This retrospective study was approved by the Ethics Committee of the Second Hospital of Lanzhou University, and the requirement for patient consent was waived.

Disclosures: The authors declare no conflict of interest.

Funding: This work was supported by the National Natural Science Foundation of China (Grant Nos. 82371969 and 82460349), the Key Science and Technology Project of Gansu Province-Social Development Category (Grant No. 232DFA006), and the Natural Science Foundation of Chongqing, China (Grant No. CSTB2024NSCQ-MSX0674).

Data and materials availability: The datasets and materials supporting these findings of this study are available from the corresponding author upon reasonable request. Patient-sensitive data will be anonymized prior to sharing to protect privacy.

Author contributions

Yuanqin Zhang (First Author): Study design, data collection and analysis, manuscript drafting.

Fang Nie (Corresponding Author): Research supervision, funding acquisition, manuscript revision and final approval.

HeYang: Technical support for experiments, data validation.

Yifei Chen: Statistical analysis, visualization.

Xiaorong Lv: Literature review, manuscript editing.

Rong Yang: Literature review, manuscript editing.

GuoChen: Literature review, manuscript editing.

All authors have read and approved the final version of the manuscript.

Acknowledgments: The authors would like to express sincere gratitude to the Department of Radiology at The Second Hospital of Lanzhou University Hospital for their technical support and clinical collaboration. We also thank all the patients who participated in this study.

Reference

1. Jaber F, Cholankeril G, El-Serag HB. Contemporary epidemiology of hepatocellular carcinoma: Understanding risk factors and surveillance strategies. Journal of the Canadian Association of Gastroenterology. 2024; 7: 331-345.
2. Zhan Z, Chen B, Huang R, et al. Long-term trends and future projections of liver cancer burden in China from 1990 to 2030. Scientific reports. 2025; 15: 13120.
3. Han B, Zheng R, Zeng H, et al. Cancer incidence and mortality in China, 2022. J Natl Cancer Cent. 2024; 4: 47-53.
4. Global incidence, prevalence, Years Lived with Disability (YLDs), Disability-Adjusted Life years (DALYs), and Healthy Life Expectancy (HALE) for 371 diseases and injuries in 204 countries and territories and 811 subnational locations, 1990-2021: A systematic analysis for the Global Burden of Disease Study 2021. Lancet. 2024; 403: 2133-2161.
5. Fattovich G, Stroffolini T, Zagni I, Donato F. Hepatocellular carcinoma in cirrhosis: Incidence and risk factors. Gastroenterology. 2004; 127: 35-50.
6. Forner A, Reig M, Bruix J. Hepatocellular carcinoma. Lancet. 2018; 391: 1301-1314.
7. Nagtegaal ID, Odze RD, Klimstra D, et al. The 2019 WHO classification of tumours of the digestive system. Histopathology. 2020; 76: 182-188.

8. Chen J, Xia C, Duan T, et al. Macro Trabecular-massive hepatocellular carcinoma: Imaging identification and prediction based on geodetic acid-enhanced magnetic resonance imaging. Eur Radial. 2021; 31: 7696-7704.

9. Fang JH, Zhou HC, Zhang C, et al. A novel vascular pattern promotes metastasis of hepatocellular carcinoma in an epithelial-mesenchymal transition-independent manner. Hepatology. 2015; 62: 452-465.

10. Feng Z, Li H, Zhao H, et al. Preoperative CT for Characterization of Aggressive Macro Trabecular-Massive Subtype and Vessels That Encapsulate Tumor Clusters Pattern in Hepatocellular Carcinoma. Radiology. 2021; 300: 219-229.

11. Tan PS, Nakagawa S, Goossens N, et al. Clinicopathological indices to predict hepatocellular carcinoma molecular classification. Liver Int. 2016; 36: 108-118.

12. Renne SL, Woo HY, Allegra S, et al. Vessels Encapsulating Tumor Clusters (VETC) Is a Powerful Predictor of Aggressive Hepatocellular Carcinoma. Hepatology. 2020; 71: 183195.

13. Mulé S, Galletto Pregliasco A, Tenenhaus A, et al. Multiphase Liver MRI for Identifying the Macro Trabecular-Massive Subtype of Hepatocellular Carcinoma. Radiology. 2020; 295: 562-571.

14. Claudon M, Cosgrove D, Albrecht T, et al. Guidelines and good clinical practice recommendations for Contrast Enhanced Ultrasound (CEUS) - update 2008. Ultra's hall in der Medizing (Stuttgart, Germany: 1980). 2008; 29: 28-44.

15. Dietrich CF, Nosler CP, Barr RG, et al. Guidelines and Good Clinical Practice Recommendations for Contrast-Enhanced Ultrasound (CEUS) in the Liver-Update 2020 WFUMB in Cooperation with EFSUMB, AFSUMB, AIUM, and FLAUS. Ultrasound in medicine & biology. 2020; 46: 2579-2604.

16. Wilson SR, Burns PN. Microbubble-enhanced US in body imaging: What role? Radiology. 2010; 257: 24-39.

17. Luo M, Liu X, Yong J, et al. Preoperative prediction of macro trabecular-massive hepatocellular carcinoma based on B-Mode US and CEUS. Eur Radial. 2023; 33: 40244033.

18. Wu J, Liu S, Zhang Y, et al. Prediction of Macro Trabecular-Massive Hepatocellular Carcinoma and Associated Prognosis Using Contrast-enhanced US and Clinical Features. Radial Imaging Cancer. 2025; 7: 240419.

19. Calderaro J, Couchy G, Imbeaud S, et al. Histological subtypes of hepatocellular carcinoma are related to gene mutations and molecular tumour classification. J Hepatol. 2017; 67:7 27738.

20. Ziol M, Poté N, Amaddeo G, et al. Macrotrabecular-massive hepatocellular carcinoma: A distinctive histological subtype with clinical relevance. Hepatology (Baltimore, Md.). 2018; 68: 103-112.

21. Sessa A, Mulé S, Brustia R, et al. Macrotrabecular-Massive Hepatocellular Carcinoma: Light and Shadow in Current Knowledge. Journal of hepatocellular carcinoma. 2022; 9: 661-670.

22. Kurebayashi Y, Sakamoto M. Macrotrabecular hepatocellular carcinoma: Unique immunovascular characteristics. Hepatology (Baltimore, Md.). 2026; 83: 203-205.

23. Kim TH, Woo S, Lee DH, Do RK, Chernyak V. MRI imaging features for predicting macro trabecular-massive subtype hepatocellular carcinoma: A systematic review and metanalysis. European radiology. 2024; 34: 6896-6907.

24. Yoo SH, Nahm JH, Chang HY, Lee JI, Lim JH, Lee HW. Macro trabecular-Massive Subtype Is Associated with a High Risk of the Recurrence of Hepatocellular Carcinoma. Journal of clinical medicine. 2026; 15.

25. Taddei TH, Brown DB, Yarchoan M, Mendiratta-Lala M, Llovet JM. Critical Update: AASLD Practice Guidance on prevention, diagnosis, and treatment of hepatocellular carcinoma. Hepatology. 2025; 82: 272-274.

26. Ridder DA, WeinmannA, Schindeldecker M, et al. Comprehensive clinicopathologic study of alpha fetoprotein-expression in a large cohort of patients with hepatocellular carcinoma. Int J Cancer. 2022; 150: 1053-1066.

27. Shan Y, Yu X, Yang Y, et al. Nomogram for the Preoperative Prediction of the Macro Trabecular-Massive Subtype of Hepatocellular Carcinoma. Journal of hepatocellular carcinoma. 2022; 9: 717-728.

28. Zhao ZC, Zheng SS, Wan YL, Jia CK, Xie HY. The molecular mechanism underlying angiogenesis in hepatocellular carcinoma: The imbalance activation of signaling pathways. Hepatobiliary Pancreatic Dis Int. 2003; 2: 529-536.

29. Tohme S, Yazdani HO, Liu Y, et al. Hypoxia mediates mitochondrial biogenesis in hepatocellular carcinoma to promote tumor growth through HMGB1 and TLR9 interaction. Hepatology. 2017; 66: 182-197.

30. Taniai T, Haruki K, Väyrynen JP, et al. Immunological and prognostic significance of Vessels Encapsulating Tumor Clusters (VETC) in hepatocellular carcinoma. Eur J Surg Oncol. 2025; 51: 110381.

31. Jang HJ, Kim TK, Burns PN, Wilson SR. Enhancement patterns of hepatocellular carcinoma at contrast-enhanced US: Comparison with histologic differentiation. Radiology. 2007; 244: 898-906.

32. Vietti Violi N, Lewis S, Hectors S, Said D, Taouli B. Radiological Diagnosis and Characterization of HCC. In: Hoshida Y, ed. Hepatocellular Carcinoma: Translational Precision Medicine Approaches. Cham (CH): Humana Press Copyright 2019, Springer Nature Switzerland AG. 2019: 71-92.

33. Sirlin CB, Kielar AZ, Tang A, Bashir MR. LI-RADS: A glimpse into the future. Abdom Radiol (NY). 2018; 43: 231-236.

34. Choi JY, Lee JM, Sirlin CB. CT and MR imaging diagnosis and staging of hepatocellular carcinoma: Part II. Extracellular agents, hepatobiliary agents, and ancillary imaging features. Radiology. 2014; 273: 30-50.

35. Yang HK, Burns PN, Jang HJ, et al. Contrast-enhanced ultrasound approach to the diagnosis of focal liver lesions: The importance of washout. Ultrasonography (Seoul, Korea). 2019; 38: 289-301.